Journal of Sound and Vibration (2000) **236**(2), 323–337
doi:10.1006/jsvi.2000.2968, available online at http://www.idealibrary.com on IDEAL®

DYNAMIC MODEL OF VIBRATION ISOLATOR UNDER STATIC LOAD

J. D. Dickens

Defence Science and Technology Organisation (DSTO), Aeronautical and Maritime Research Laboratory (AMRL), P.O. Box 4331, *Melbourne, Victoria* 3001, *Australia*

(*Received* 14 *April* 1999, *and in final form* 3 *February* 2000)

This study investigates a dynamic model of a vibration isolator as a function of the compression ratio of its rubber element. The model is in terms of the four-pole parameters, and is based on a relationship between the phase velocity and compression ratio of the rubber element proposed in a companion publication. Experimental data are presented for both unfilled and filled natural rubbers, which shows satisfactory agreement with the model. The agreement is improved by the inclusion of a correction factor.

1. INTRODUCTION

In the companion paper [1], a model was proposed that predicts the effect of the static compression on the phase velocity in the rubber element of a vibration isolator. This may be used in the dynamic model developed by Snowdon [2, 3] to predict the four-pole parameters of a vibration isolator in terms of its compression ratio. The compression ratio of a vibration isolator is defined as the static compressed height of the rubber element under load, divided by its uncompressed height. The compression ratio of an unloaded vibration isolator is therefore unity. This study is concerned with unfilled and filled natural rubber vulcanisates, with the commonly used filler carbon black.

The notation followed represents complex numbers with the superscript *, and real numbers are not superscripted. Imaginary components are represented using $\mathrm{j} = \sqrt{-1}$. In the contemporary literature, the commonly used symbols for the compression ratio and wavelength are both lambda, λ. This study does not use the wavelength, and so denotes the compression ratio by the symbol λ.

The vibration isolator is considered to comprise a resilient element of homogeneous rubber that is securely bonded to two end plates. The end plates are used for attaching the vibration isolator to the upper and lower structures, and are assumed to have no structural modes in or near the frequency of interest. The undeformed rubber element is assumed to have a regular right prismatic shape. Let the top plate, rubber element and bottom plate have masses m_T, m_R and m_B respectively. The unloaded vibration isolator has an undeformed rubber element of height h_0, cross-sectional area A_0 and shape factor S. The shape factor is defined as the ratio of the loaded area at one end to the total force-free area of the undeformed rubber element [4, 5].

Let the phase velocity for an undeformed long rod of the same rubber as the vibration isolator under consideration be c_0^*. A long rod is defined to be a rod that has lateral dimensions small compared to the longitudinal wavelength, and quantitatively the lateral dimensions should be less than one-tenth of the wavelength [6]. The terms "bar" and

0022-460X/00/370323 + 15 $35.00/0

"beam" are also used by other authors for the word "rod". Let the undeformed rubber have complex normal modulus E_0^*, loss angle δ_0, loss factor $\tan\delta_0$, density ρ and the Poisson ratio v. Let the magnitude of the complex normal modulus be E_0. Then

$$E_0^* = E_0 e^{j\delta_0} \tag{1}$$

and from the wave equation the phase velocity for the undeformed long rod c_0^* is

$$c_0^* = \sqrt{\frac{E_0^*}{\rho}}. \tag{2}$$

Let a static load be applied to the vibration isolator, which compresses the rubber element to a barrel shape of compression ratio λ, radius of gyration r_G and height h. Under deformation, the rubber element is assumed to have a regular right barrel shape with parallel ends. The compressed height is

$$h = \lambda h_0. \tag{3}$$

Let the compressed rubber have complex normal modulus E_D^*, loss angle δ and loss factor $\tan\delta$. The density and the Poisson ratio are assumed to be the same as for the undeformed rubber, namely ρ and v respectively. Let the longitudinal wave propagated within the compressed rubber element have circular frequency ω and phase velocity c_C^*. Then the phase velocity is given by the companion paper [1] as

$$c_C^* = \left\{\frac{(1+\beta S^2)(2+\lambda^3)[(c_0^*)^2 - (\omega v r_G)^2]}{3\lambda}\right\}^{1/2}, \tag{4}$$

where β is a constant.

The parameter β is a numerical constant for a given rubber, and its values have been tabulated for different hardness values of rubbers [7].

For the case of a vibration isolator with a cylindrical rubber element of undeformed radius r_0, the shape factor is [1]

$$S = \frac{r_0}{2h_0} \tag{5}$$

and the phase velocity is given by the companion paper [1] as

$$c_C^* = \frac{\{(1+\beta S^2)(2+\lambda^3)[8\lambda(c_0^*)^2 - (\omega r_0)^2]\}^{1/2}}{2\sqrt{6}\lambda}. \tag{6}$$

Equations (4) and (6) embody correction factors for the static compressive effects on the phase velocity of longitudinal wave propagation in a short rubber rod compressed with a barrel shape. They were based on the notion of an effective rubber cylinder and applicable to natural rubber vulcanisates, unfilled or filled with carbon black.

2. MODEL OF VIBRATION ISOLATOR

In this section the proposed equation (4) is applied to the four-pole parameters of a vibration isolator under static compression. Let the vibration isolator have an input force and velocity designated by F_1^* and V_1^*, respectively, and an output force and velocity

F_2^* and V_2^* respectively. Let the four-pole parameters of the vibration isolator be α_{11}^*, α_{12}^*, α_{21}^* and α_{22}^*, which are complex, time-invariant functions of the circular frequency ω. The four-pole parameters relate the input and output forces and velocities of the vibration isolator and are defined by [8]

$$\begin{bmatrix} F_1^* \\ V_1^* \end{bmatrix} = \begin{bmatrix} \alpha_{11}^* & \alpha_{12}^* \\ \alpha_{21}^* & \alpha_{22}^* \end{bmatrix} \begin{bmatrix} F_2^* \\ V_2^* \end{bmatrix}. \tag{7}$$

Applying Snowdon's [2, 3] derivation of the four-pole parameters to the current situation gives

$$\alpha_{11}^* = \cos\theta^* - \gamma_1 \theta^* \sin\theta^*, \tag{8}$$

$$\alpha_{12}^* = \mu_R^* [(\sin\theta^* + \gamma_1 \theta^* \cos\theta^*) + \gamma_2 \theta^* (\cos\theta^* - \gamma_1 \theta^* \sin\theta^*)], \tag{9}$$

$$\alpha_{21}^* = -\frac{\sin\theta^*}{\mu_R^*} \tag{10}$$

and

$$\alpha_{22}^* = \cos\theta^* - \gamma_2 \theta^* \sin\theta^*, \tag{11}$$

where

$$\theta^* = \frac{\omega\lambda h_0}{c_C^*}, \qquad \mu_R^* = \frac{\mathrm{j}\omega m_R}{\theta^*}, \tag{12, 13}$$

$$\gamma_1 = \frac{m_T}{m_R} \tag{14}$$

and

$$\gamma_2 = \frac{m_B}{m_R}. \tag{15}$$

The proposed static compression model is embodied in equations (4) and (7)–(15), and predicts the four-pole parameters for low frequencies.

3. VIBRATION ISOLATORS A AND B

Two large cylindrical vibration isolators were manufactured [9] and are designated A and B. Vibration isolator A had a rubber element composed of an unfilled natural rubber vulcanisate. Vibration isolator B had a rubber element composed of a natural rubber vulcanisate filled with carbon black. The formulations are given in Table A1 of Appendix A.

The undeformed rubber diameter of vibration isolator A varied from 170·0 mm at the ends to 167·4 mm at its centre. For vibration isolator B, the undeformed rubber diameter varied from 170·0 mm at the ends to 168·2 mm at its centre. The undeformed radius r_0 is taken as the average value of the radii at an end and the centre. The hardness was measured using a hand-held pocket type of durometer (rubber hardness meter). This meter measured the surface hardness and ideally required a flat surface for measurement, whereas both rubber elements were curved. The hardness values measured by this method were approximate, and assumed that the rubber elements were uniform throughout. The measured geometric parameters, including the hardness measured in International Rubber Hardness degrees (IRHD), are presented in Table 1.

TABLE 1

Measured geometric properties of vibration isolators A and B

Vibration isolator	h_0 (m)	r_0 (m)	S	Hardness (IRHD)	β	$(1 + \beta S^2)$
A	0·1478	$8{\cdot}43 \times 10^{-2}$	0·285	47	1·54	1·13
B	0·1499	$8{\cdot}45 \times 10^{-2}$	0·282	64	1·10	1·09

TABLE 2

Measured mass properties of vibration isolators A and B

Vibration isolator	m_T (kg)	m_B (kg)	m_R (kg)	Total mass (kg)	ρ (kg/m^3)
A	1·306	1·306	3·160	5·772	971
B	1·308	1·308	3·540	6·156	1063

TABLE 3

Measured rubber properties of vibration isolators A and B

Vibration isolator	f_{AV} (Hz)	E_0 (Pa)	$\tan \delta_0$	ρ (kg/m^3)	c_0 (m/s)
A	81	$2{\cdot}44 \times 10^6$	3×10^{-2}	971	50·1
B	121	$5{\cdot}53 \times 10^6$	4×10^{-2}	1063	72·1

The masses m_T and m_B were measured prior to manufacture of the vibration isolators. The densities were calculated from the compositions of the rubbers used and checked by measurements. The measured mass properties are presented in Table 2.

The undeformed complex normal modulus E_0^* of the rubber element of each vibration isolator was measured using a resonance technique with different end masses to determine the mass contribution of the rubber element [9]. The average frequency of measurement was f_{AV} and the magnitude of the phase velocity c_0 is given from equation (2). The measured rubber properties are presented in Table 3.

4. MEASUREMENT OF FOUR-POLE PARAMETERS

The vibration isolator test facility [9] was used to measure the four-pole parameters of vibration isolators A and B under different compression ratios. The vibration isolator test facility had a lower limit of 5 Hz, which was selected for the tests.

Before each set of tests, each vibration isolator was mechanically conditioned by loading and unloading it six times up to the maximum testing static plus dynamic strain plus 10% [10]. After being mechanically conditioned, each vibration isolator was thermally conditioned by maintaining it at 20°C for a duration of at least 18 h before testing, and then

tested at the same temperature. The tolerance on the conditioning and testing temperature was $\pm 1^{\circ}$C.

The dynamic testing comprised the application of a sinusoidal force that was linearly swept over the frequency range of interest with 0·5 Hz steps. At each forcing frequency 16 cycles were applied before the measurements were conducted. The dynamic strains of the rubber elements did not exceed 1×10^{-3}, and thus their complex normal moduli may be treated as constant [11, 12]. At each test frequency the data were averaged over 32 cycles.

The compression ratio λ was calculated as the ratio of the compressed to undeformed heights of the rubber element. Experimentally, the compressed height was determined as the average of four heights, measured vertically and equally spaced around the vibration isolator. For each test, the accuracy of the compressed height along the longitudinal axis of the vibration isolator was $\pm 0{\cdot}5$ mm, which with the minimum compression ratio of 0·80 represented $\pm 0{\cdot}5$ in 120 mm, i.e., $\pm 0{\cdot}4\%$.

For each test, the compressed ends of the vibration isolator were equally spaced to within 0·25 mm, measured as the height between the end plates. Since the diameters of the end plates were 150 mm, the maximum vertical misalignment between the end plates was $2 \times 0{\cdot}25$ mm/150 mm, i.e., $0{\cdot}2^{\circ}$.

4.1. FIRST ANTI-RESONANCE OF α_{11}^* AND α_{22}^*

Each vibration isolator had end plates of equal mass, a uniform shape and the rubber element was assumed to be homogeneous. Hence each vibration isolator is assumed to be symmetrical, and so its four-pole parameters α_{11}^* and α_{22}^* are identical [2, 3].

Dickens [9] developed a method of using the first anti-resonant behaviour of the four-pole parameters α_{11}^* and α_{22}^* of a symmetrical vibration isolator under static load as a measure of the accuracy of the predicted loss factor and magnitude of the phase velocity calculated from equation (4).

Let the frequency and magnitude of the four-pole parameters α_{11}^* and α_{22}^* at their first anti-resonance troughs be f_0 and U_0 respectively. Then, as an approximation [9]

$$\tan \delta = U_0. \tag{16}$$

The measured and predicted magnitudes of the four-pole parameters α_{11}^* and α_{22}^* at their first anti-resonance troughs may therefore be used as a comparative measure of the loss factor accuracy of equation (4).

The magnitude of the phase velocity is proportional to the frequency f_0 [9]. The measured and predicted frequencies of the first anti-resonances of the four-pole parameters α_{11}^* and α_{22}^* may thus be employed as a comparative measure of the magnitude accuracy of the phase velocity calculated from equation (4).

4.2. VIBRATION ISOLATOR A

In this section a comparison is made between the measured and predicted four-pole parameters of vibration isolator A over the compression ratios from 0·98 to 0·70.

For a maximum error in the phase velocity reduction factor of 10%, the maximum diameter-to-wavelength ratio is 1·41, where the diameter is that of the effective rubber cylinder [1]. Figure 1 shows the effective diameter-to-wavelength ratio of the vibration isolator A for the compression ratios tested. It indicates that for a frequency of 220 Hz, the diameter-to-wavelength ratio varies from 1·3 to 4·3. Therefore, as a compromise the upper

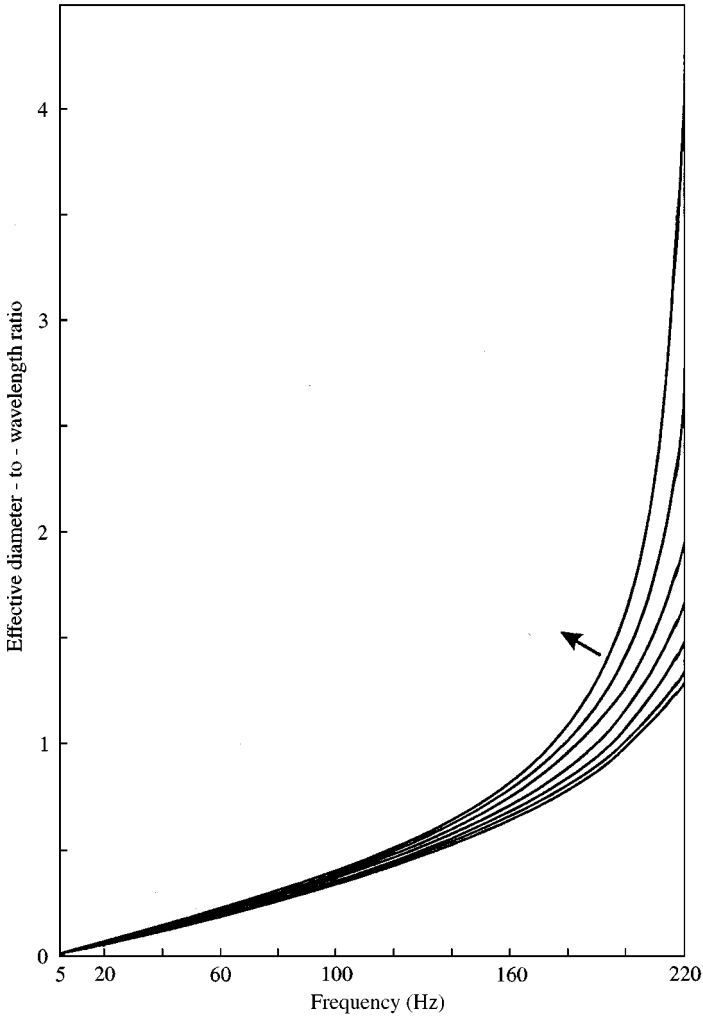

Figure 1. Effective diameter-to-wavelength ratio for vibration isolator A. Arrow shows decreasing λ: 0·97, 0·95, 0·90, 0·85, 0·80, 0·75 and 0·70.

limit of 220 Hz was selected for the tests. Over the compression ratio tested, the model should be valid up to a frequency of approximately 190 Hz.

The measured and predicted four-pole parameters using equations (6)–(15) are presented in Figures 2–7. Comparing these figures shows that the general shapes of the measured and predicted four-pole parameters are the same up to a frequency of approximately 190 Hz. For frequencies up to approximately 100 Hz, the agreement is better than for the higher frequencies.

Consider the application of section 4.1 to the first anti-resonant behaviour of the four-pole parameters α_{11}^* and α_{22}^*, which from Figure 2 occurs around the frequency of 70 Hz. The measured and predicted four-pole parameters α_{11}^* and α_{22}^* are presented in Figures 2 and 5 respectively. These figures show that the magnitudes of the predicted and measured four-pole parameters α_{11}^* and α_{22}^* at their first anti-resonance troughs are constant and equal to each other within 1 dB. Hence from equation (16) it is considered that

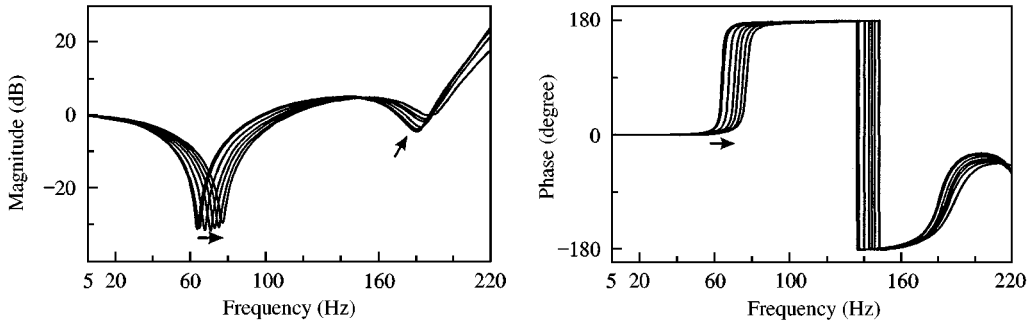

Figure 2. Measured four-pole parameters α_{11}^* and α_{22}^* for vibration isolator A. Arrows show decreasing λ: 0·97, 0·95, 0·90, 0·85, 0·80, 0·75 and 0·70.

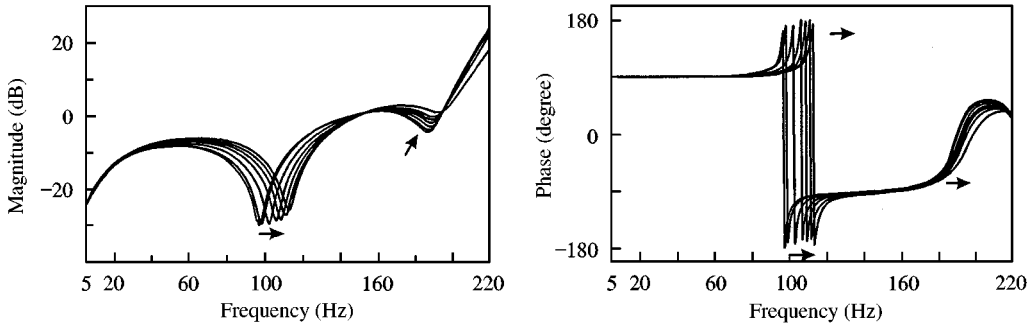

Figure 3. Measured four-pole parameters α_{12}^* for vibration isolator A. Arrows show decreasing λ: 0·97, 0·95, 0·90, 0·85, 0·80, 0·75 and 0·70.

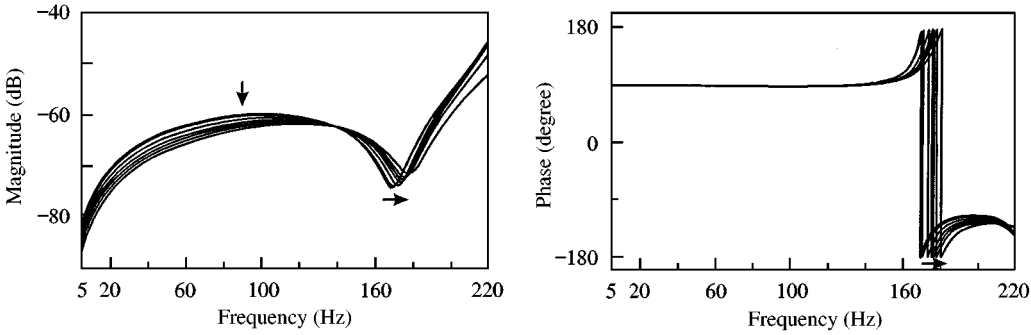

Figure 4. Measured four-pole parameters α_{21}^* for vibration isolator A. Arrows show decreasing λ: 0·97, 0·95, 0·90, 0·85, 0·80, 0·75 and 0·70.

the loss factor of the vibration isolator remains constant for compression ratios from 0·97 to 0·07, and the predicted and measured values agree.

Figures 2 and 5 show that the percentage magnitude difference between the predicted and measured frequencies monotonically increases as the compression ratio decreases, and reaches a maximum of 15 referenced to the measured value, at a compression ratio of 0·70. For compression ratios down to 0·80, the magnitude difference in frequencies attains a maximum value of 6·6% at a compression ratio of 0·80.

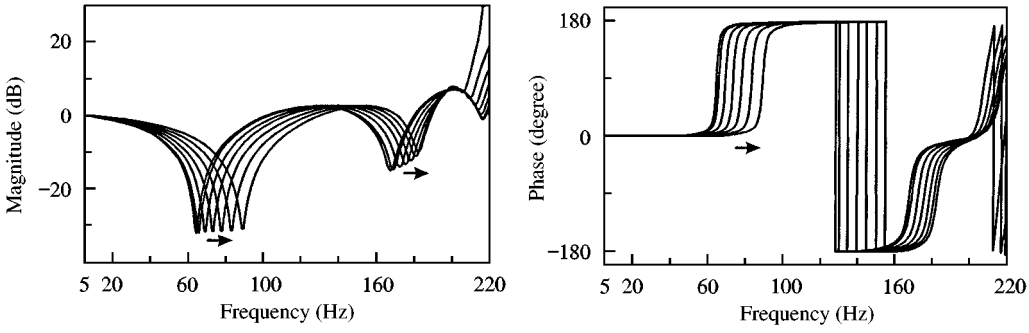

Figure 5. Predicted four-pole parameters α_{11}^* and α_{22}^* for vibration isolator A. Arrows show decreasing λ: 0·97, 0·95, 0·90, 0·85, 0·80, 0·75 and 0·70.

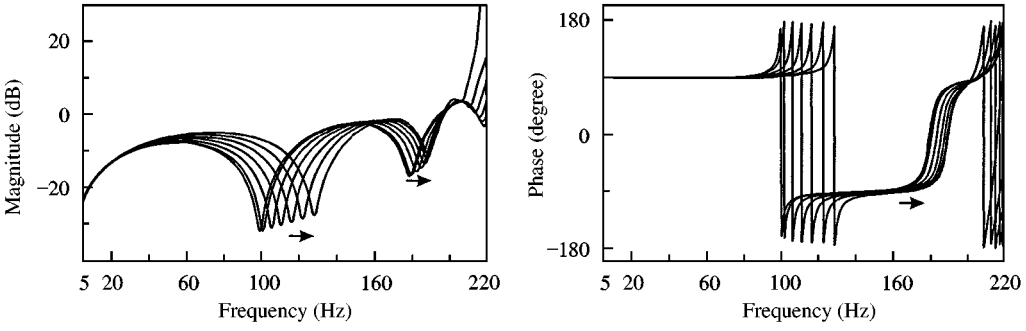

Figure 6. Predicted four-pole parameter α_{12}^* for vibration isolator A. Arrows show decreasing λ: 0·97, 0·95, 0·90, 0·85, 0·80, 0·75 and 0·70.

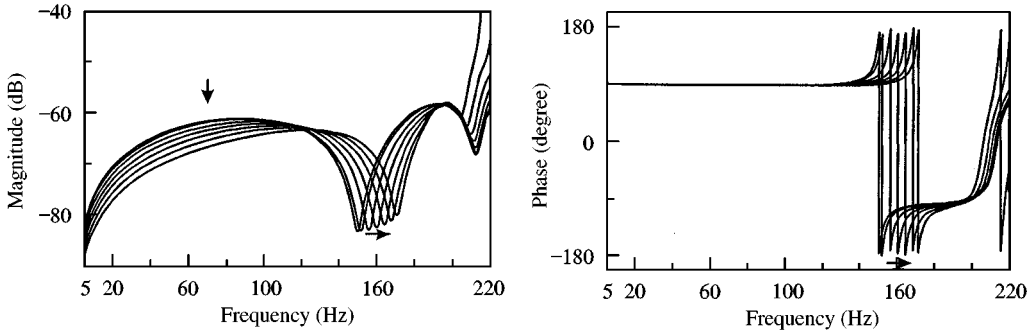

Figure 7. Predicted four-pole parameter α_{21}^* for vibration isolator A. Arrows show decreasing λ: 0·97, 0·95, 0·90, 0·85, 0·80, 0·75 and 0·70.

Note that the anti-resonance troughs of the four-pole parameters α_{11}^* and α_{22}^* correspond to maxima in the magnitudes of the blocked force transmissibility. The first maximum in the magnitude of the blocked force transmissibility is the resonance of the top plate on the rubber element of the blocked vibration isolator, and maxima at higher frequencies correspond to standing waves in the rubber element. Consequently the first standing wave frequency is approximately 180 Hz for vibration isolator A (Figure 2).

4.3. VIBRATION ISOLATOR B

In this section a comparison is undertaken of the measured and predicted four-pole parameters of vibration isolator B over the compression ratios from 0·98 to 0·80.

Figure 8 shows the effective diameter-to-wavelength ratio for the compression ratios tested. It indicates that for a frequency of 320 Hz, the diameter-to-wavelength ratio varies from 1·3 to 2·2. Similar to section 4.2, the upper limit of 320 Hz was selected as a compromise for the tests. Over the compression ratios tested, the model should be valid up to a frequency of approximately 290 Hz.

The measured and predicted four-pole parameters for vibration isolator B are presented in Figures 9–14. Comparing these figures shows that the general shapes of the measured and predicted four-pole parameters are the same up to a frequency of approximately 290 Hz. For frequencies up to approximately 180 Hz, the agreement is better than for the higher frequencies.

Figures 9 and 12 show that the percentage difference between the measured and predicted frequencies of the first anti-resonance troughs of the four-pole parameters α_{11}^{*} and

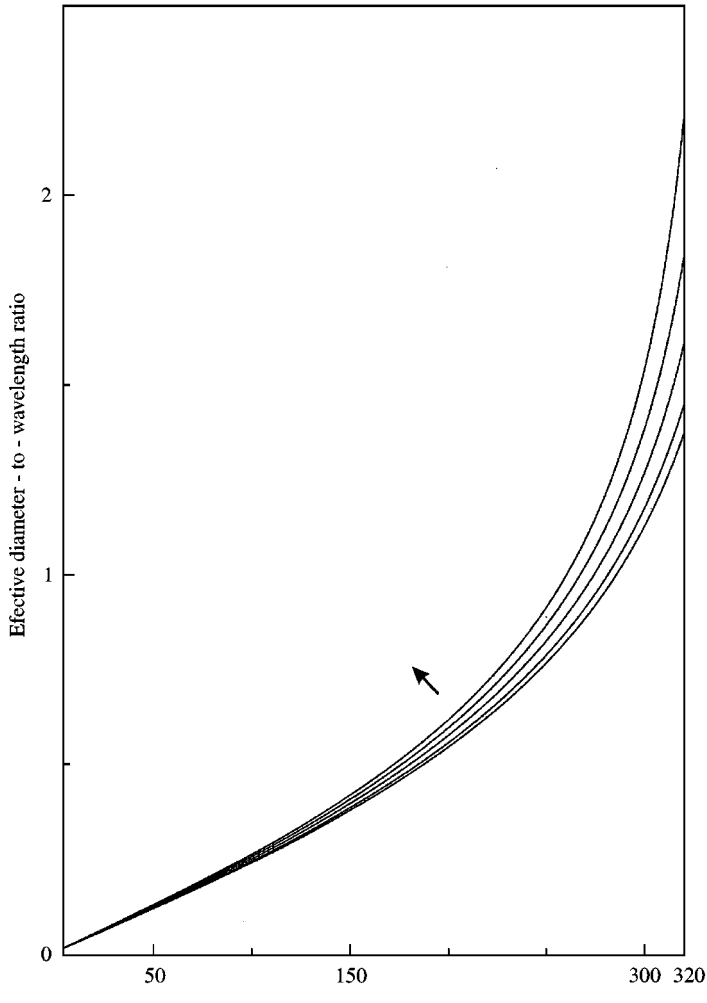

Figure 8. Effective diameter-to-wavelength ratio for vibration isolator B. Arrow shows decreasing λ: 0·98, 0·95, 0·90, 0·85 and 0·80.

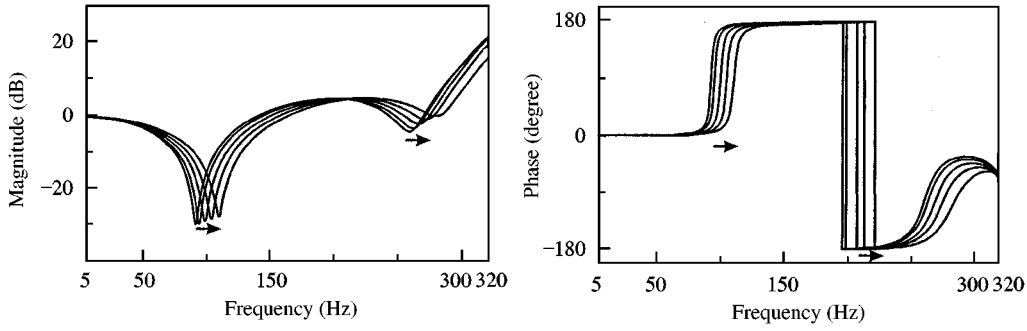

Figure 9. Measured four-pole parameters α_{11}^* and α_{22}^* for vibration isolator B. Arrows show decreasing λ: 0·98, 0·95, 0·90, 0·85 and 0·80.

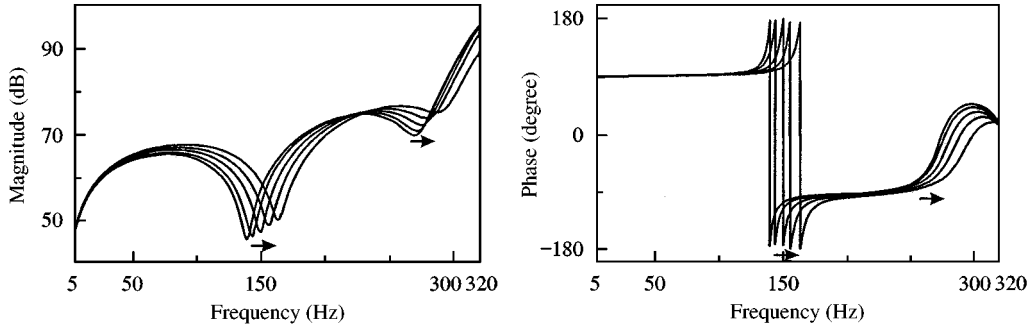

Figure 10. Measured four-pole parameter α_{12}^* for vibration isolator B. Arrows show decreasing λ: 0·98, 0·95, 0·90, 0·85 and 0·80.

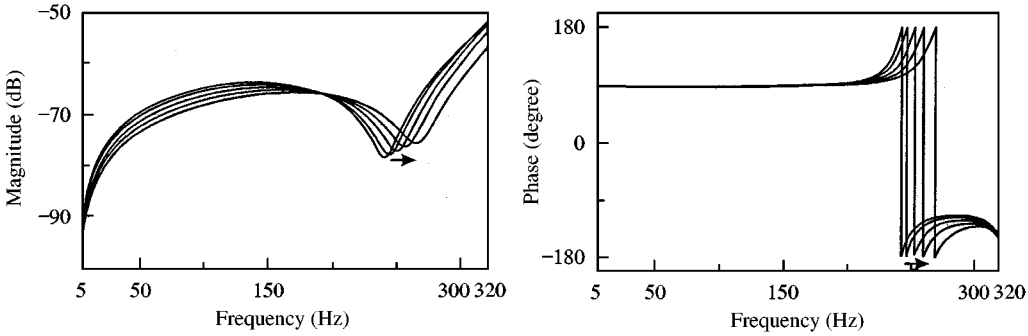

Figure 11. Measured four-pole parameter α_{21}^* for vibration isolator B. Arrows show decreasing λ: 0·98, 0·95, 0·90, 0·85 and 0·80.

α_{22}^* reaches a maximum of 1·7 referenced to the measured value, at a compression ratio of 0·80.

Inspection of Figure 12 reveals that magnitudes of the predicted four-pole parameters α_{11}^* and α_{22}^* at their first anti-resonance troughs are approximately constant. However, the measured magnitudes increase significantly with decreasing compression ratio. Thus, from equation (16) the measured loss factor increases as the compression ratio decreases. Over the compression ratio range from 0·98 to 0·80, the measured loss factor increases by 2·62 dB.

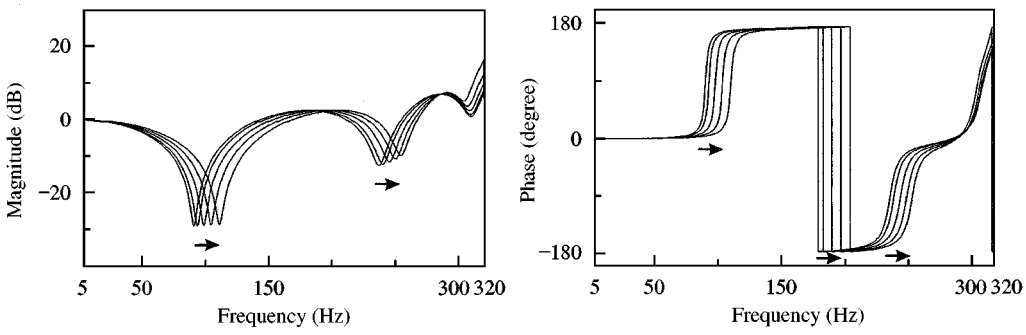

Figure 12. Predicted four-pole parameter α_{11}^* and α_{22}^* for vibration isolator B. Arrows show decreasing λ: 0·98, 0·95, 0·90, 0·85 and 0·80.

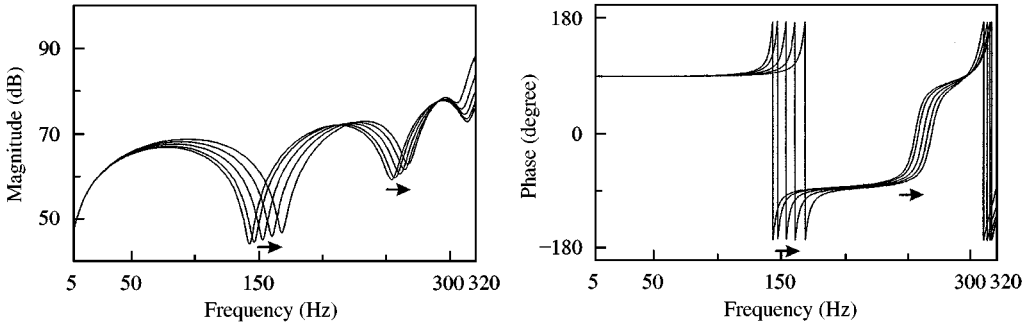

Figure 13. Predicted four-pole parameter α_{12}^* for vibration isolator B. Arrows show decreasing λ: 0·98, 0·95, 0·90, 0·85 and 0·80.

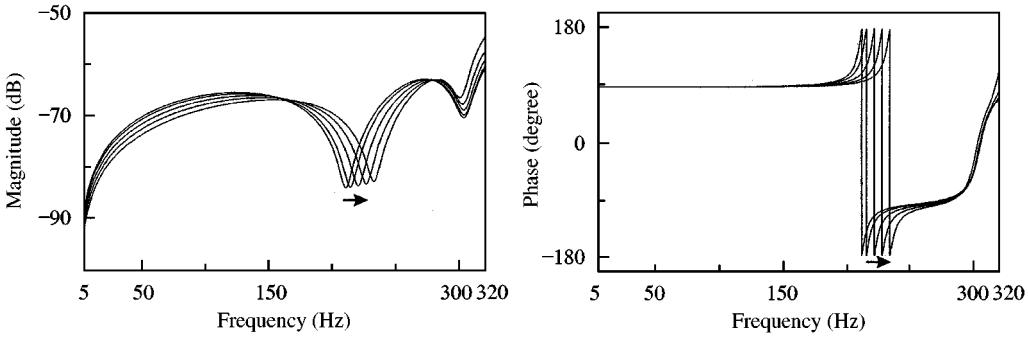

Figure 14. Predicted four-pole parameter α_{21}^* for vibration isolator B. Arrows show decreasing λ: 0·98, 0·95, 0·90, 0·85 and 0·80.

4.4. IMPROVED STATIC COMPRESSION MODEL

For compression ratios down to 0·8 the model satisfactorily predicted the low frequency behaviour of vibration isolators A and B (sections 4.2 and 4.3). However, it may be improved by including a correction factor to account for the observed experimental behaviour of the vibration isolators.

During the tests of each of the vibration isolator A and B the temperature remained constant, the same procedure was used and it is assumed that the complex normal modulus

of the rubber element remained constant over the range of testing frequencies. Therefore, the only parameter that varied for the different vibration isolator tests was the compression ratio. This implies that the correction factor is a function of the compression ratio only. Equation (6) is thus modified by the inclusion of a correction factor p^* and becomes

$$c_C^* = \frac{\{p^*(1+\beta S^2)(2+\lambda^3)[8\lambda(c_0^*)^2 - (\omega r_0)^2]\}^{1/2}}{2\sqrt{6}\lambda}, \tag{17}$$

where $p^* = p^*(\lambda)$.

For vibration isolator A, the loss factor was constant and so the correction factor is real and $p^* = p$. The values of p were determined by iteration so that equation (17) produced the same first anti-resonance frequencies as those measured. Figure 15 shows a plot of p and a regression curve based on a polynomial of order 4, for vibration isolator A.

For vibration isolator B, the values of p^* were determined by iteration so that equation (17) produced the same first anti-resonance frequencies and magnitudes as those measured. Figure 16 shows a plot of p^* and a regression curve based on a polynomial of order 4 for the magnitude, and a linear regression for the phase. The phase of p^* is approximately equal to the apparent increase in the loss factor of the compressed rubber element, and is thus shown in radians (Figure 16).

Incorporating these correction factors significantly improved the overall agreement between the predicted and measured four-pole parameters of both vibration isolators.

4.5. COMPARISON WITH PREVIOUS RESEARCH

A literature search indicated that the only relevant reference is Andersson [13], because it is the only one that specifically addresses the effect of static load on the wave effects of vibration isolators.

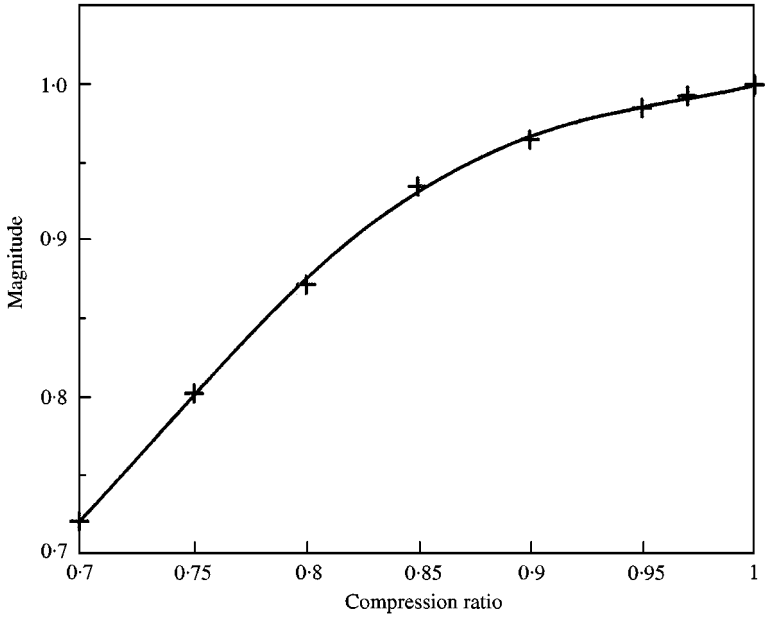

Figure 15. Measured correction factor p for vibration isolator A.

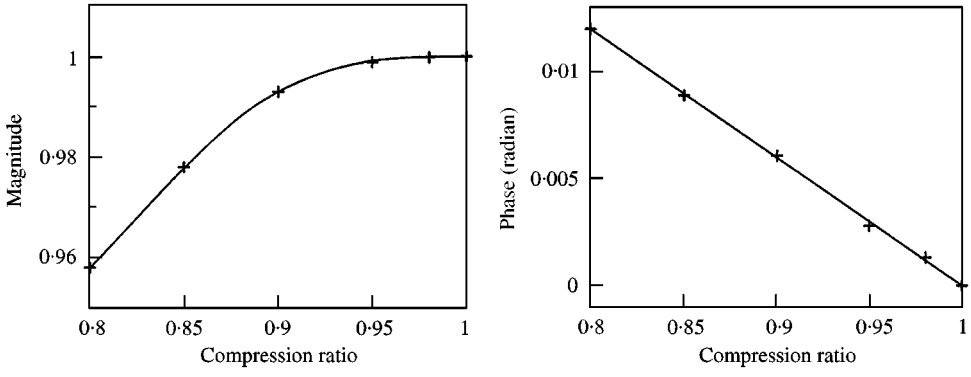

Figure 16. Measured correction factor p^* for vibration isolator B.

Andersson [13] investigated a small vibration isolator with a rubber element composed of an unspecified "soft natural rubber" of hardness 40 IRHD. The vibration isolator was in the form of a rectangular regular prism of dimensions 100 mm (length) × 70 mm (width) × 105 mm (height). The vibration isolator was tested in compression and for different compression ratios he measured the magnitude of the blocked impedance. Andersson presented plots of the magnitude of the blocked impedance over the frequency range from 30 to 700 Hz for compression ratios of 0·96 and 0·80, and from 40 to 800 Hz for a compression ratio of 0·60. These frequency ranges excluded the resonance of the top plate on the rubber element, and showed all of the first two standing waves resonance peaks.

The four-pole parameter α_{21}^* is equal to the reciprocal of the impedance, for the blocked output situation [9]. Andersson assumed that his tests were conducted with a blocked output. Therefore, the magnitude of the four-pole parameter α_{21}^* was calculated from his results. The general shape of the curves of the calculated magnitude of the four-pole parameter α_{21}^*, as a function of frequency, agreed with the shapes measured in sections 4.2 and 4.3. His results showed that the frequency of the first standing wave resonance increased with decreasing compression ratio, in agreement with the findings of sections 4.2 and 4.3. His results exhibited an increase in the loss factor of the first standing wave resonance as the compression ratio diminished, in agreement with the findings of sections 4.2 and 4.3.

The results of Andersson also indicated that the magnitude of the four-pole parameter α_{21}^*, at the first standing wave resonance, increased from the compression ratio of 0·96 to 0·80, but marginally decreased from the compression ratio of 0·80 to 0·60. The increase, but not the decrease, agrees with the findings of sections 4.2 and 4.3. A possible explanation for the disagreement is the fact that the tested vibration isolators had different shapes and sizes, and that the results included a compression ratio of 0·60. This compression ratio would have induced considerable distortion into the rubber element, which may have caused the unexpected result.

Another noteworthy point is that the difference in the magnitudes of the four-pole parameter α_{21}^*, at the first standing wave resonances was only approximately 0·5 dB, for compression ratios of 0·80 and 0·60. This difference could have been attributable to experimental error, a subject not discussed by Andersson. For example, a reasonable error of $\pm$ 1 dB in the results could conceivably yield a true decrease the magnitude of the four-pole parameter α_{21}^*, at the first standing wave resonance, by 1·5 dB from the compression ratio of 0·80 to 0·60.

In summary, it may be said that the experimental results of Andersson in general agreed with the observed trends in the measured magnitude of the four-pole parameter α_{21}^*.

5. CONCLUSIONS

The static compression model embodied in equations (4) and (7)–(15) was proposed. Experimental results were obtained for two large cylindrical vibration isolators, one with a rubber element composed of an unfilled natural rubber vulcanisate and the other with a rubber element composed of a natural rubber vulcanisate filled with carbon black. The unfilled and filled vibration isolators were tested with compression ratios down to 0·70 and 0·80 respectively. Using the static compression model the general shapes of the measured and predicted four-pole parameters for each vibration isolator were the same up to a frequency with a maximum diameter-to-wavelength ratio of nominally 1·41. The agreement improved with decreasing diameter-to-wavelength ratio. Vibration isolators are commonly used over the range of compression ratios from 0·95 to 0·80, and over this range the model satisfactorily predicted the low-frequency behaviour.

A study of the predicted and measured first anti-resonance troughs of the four-pole parameters α_{11}^* and α_{22}^* was undertaken for compression ratios down to 0·80. It showed that the agreement between the predicted and measured magnitudes and anti-resonant frequencies could be improved by the addition of a correction factor to give equation (17). The loss factor of the unfilled vibration isolator remained approximately constant, while that of the filled vibration isolator increased with decreasing compression ratios. Thus, the correction factor was real for the unfilled vibration isolator and complex for the filled vibration isolator. For both vibration isolators, the magnitude of the correction factor monotonically decreased from unity with decreasing compression ratio, and could be represented as a fourth order polynomial of the compression ratio. The phase of the factor was linearly related to the compression ratio for the filled vibration isolator.

The model with the correction factor significantly improved the overall agreement between the predicted and measured four-pole parameters of both vibration isolators.

ACKNOWLEDGMENT

The author gratefully acknowledges Dr Chris Norwood, Maritime Platforms Division, DSTO, and Dr Hugh Williamson from the University of New South Wales, for discussions on themes of this paper, as well as Mr Ted Symes, Maritime Platforms Division, DSTO, for formulating and manufacturing the two vibration isolators. He also appreciates the support of AMRL during this study, as part of the work for a Ph.D. from the University of New South Wales.

REFERENCES

1. J. D. DICKENS 2000 *Journal of Sound and Vibration* **234**, 21–42. Phase velocity of rubber element in vibration isolator under static load.
2. J. C. SNOWDON 1979 *Journal of the Acoustical Society of America* **66**, 1245–1274.
3. J. C. SNOWDON 1979 *National Bureau of Standards Handbook*, Vol. 128. Applied Research Laboratory, Pennsylvania State University. Vibration isolation: use and characterisation.
4. W. C. KEYS 1937 *Mechanical Engineering* **59**, 345–349. Rubber springs.
5. E. G. KIMMICH 1940 *India Rubber World* **103**, 45–50. Rubber in compression.
6. C. H. HANSEN and S. D. SNYDER 1997 *Active Control of Noise and Vibration*. London: E & FN Spon.

7. P. B. LINDLEY 1964 *Malaysian Rubber Producers' Research Association NR Technical Bulletin, Hertfordsire*. Engineering design with natural rubber.
8. MOLLOY 1957 *Journal of the Acoustical Society of America* **29**, 842–853. Use of four-pole parameters in vibration calculations.
9. J. D. DICKENS 1998 *Ph.D. thesis, University of New South Wales, Canberra*. Dynamic characterisation of vibration isolators.
10. BS 903:A24:1992 *British Standards Association, London*. Physical testing of rubber, Part A24: guide to the determination of dynamic properties of rubbers.
11. A. R. PAYNE 1956 *Journal of Applied Polymer Science* **33**, 432. A note on the existence of a yield point in the dynamic modulus of loaded vulcanizates.
12. A. R. PAYNE and J. R. SCOTT 1960 *Engineering Design with Rubber*. London: MacLaren & Sons.
13. A. ANDERSSON 1965 *Proceedings of 5th International Congress on Acoustics, Cambridge, U.S.A.*, 7–14. *September*, L16/L16/4. Measurement of the dynamic properties of vibration isolators with varying static deformation.
14. ASTM D3853-96 1996 *American Society for Testing and Materials Standard, Philadelphia*. Standard terminology relating to rubber and rubber latices – abbreviations for chemicals used in compounding.
15. ASTM D1765-96 1996 *American Society for Testing and Materials Standard, Philadelphia*. Standard classification system for carbon blacks used in rubber products.

APPENDIX

TABLE A1

Compositions of vibration isolators A and B

Constituent*	A (phr)	B (phr)
Natural rubber, standardized Malaysian rubber (SMR) latex grade L	100·00	100·00
Zinc oxide	5·00	5·00
Stearic acid	2·50	2·50
2,2,4-Trimethyl-1,2-dihydroquinoline (oligomer) (TMQ)	2·00	2·00
Carbon black, N550 (previously termed fast extrusion furnace)	0·00	26·00
Sulphur	1·00	1·00
N-Cyclohexyl-2-benzothiazolesulfenamide (CBS)	1·70	0·26
2-(Morpholinothio)benzothiazole (MBS)	0·00	1·44
Tetramethylthiuram disulfide (TMTD)	0·30	0·30
N,*N*′-Dimethyl-*N*,*N*′ diphenyl thiuram disulphide (MPTD)	0·45	0·45
Total	112·95	138·95

Note: The abbreviations of the constituents are given by standards [14, 15].